

Shapiro-like Resonance in Ultracold Molecule Production via an Oscillating Magnetic Field

Bin Liu,^{1,2} Li-Bin Fu,^{1,3} and Jie Liu^{1,3,*}

¹*Institute of Applied Physics and Computational Mathematics, Beijing 100088, China*

²*Graduate School, China Academy of Engineering Physics, Beijing 100088, P. R. China*

³*Center for Applied Physics and Technology, Peking University, 100084, Beijing, P. R. China*

We study the process of production of ultracold molecules from ultracold atoms using a sinusoidally oscillating magnetic field modulation. When the magnetic field is resonant roughly with the molecular binding energy, Shapiro-like resonances are observed. Their resonance profiles are well fitted by the Lorentzian functions. The line widths depend on both the amplitude and the duration of the applied modulations, and are found to be dramatically broadened by thermal dephasing effect. The resonance centers shift due to both many-body effect and finite temperature effect. Our theory is consistent with recent experiment (S. T. Thompson, E. Hodby, and C. E. Wieman, Phys. Rev. Lett. **95**, 190404 (2005)). Our model predicts a 1/3 ceiling for the molecular production yield in uncondensed ultracold atomic clouds for a long coupling time, while for the condensed atoms the optimal conversion yield could be beyond the limit.

PACS numbers: 03.75.Nt, 34.50.-s, 36.90.+f

I. INTRODUCTION

Shapiro resonance is one of the most remarkable properties of the superconducting device, in which, two weakly coupled superconductors are subject to a voltage difference that is the sum of a dc component V and a periodic signal $V_m \sin(ft)$. A continuous range of nonzero dc currents are possible if $V = \frac{\hbar}{2e}kf$, where $2e$ is the Cooper pair charge, \hbar is the reduced Planck constant, and k is an integer[1, 2]. The Shapiro resonance provides a method to measure the constant of nature $2e/\hbar$ with such precision and universality[3, 4] that, since 1972, the reversed view has been adopted whereby $2e/\hbar$ is assumed to be known and the above Shapiro resonance is used to define a standard unit of voltage[2, 5, 6].

Essentially, the Shapiro resonance is a specific phenomenon emerged when the frequency of the external field is commensurate with the intrinsic frequency of system. Recently, it has received renewed interests and investigations in the Bose-Einstein condensates(BEC)[7, 8, 9]. For example, in BEC Josephson junction, the dc value of the drift current shows up as resonant spikes[7]. Under experimentally accessible conditions there exist well-developed half-integer Shapiro-like resonances[8]. Shapiro effect also allows precise measurements in atomic BECs. The ac-driven atomic Josephson devices can be used to define a standard of chemical potential[9].

In the present paper, we extend to investigate the Shapiro resonance effects in ultracold molecule production. The conversion of ultracold atoms to ultracold molecules by time varying magnetic fields in the vicinity of a Feshbach resonance is currently a topic of much experimental and theoretical interest. This particular con-

version process lends itself well to the formation of molecular Bose-Einstein condensates (BECs)[10, 11, 12, 13] and atom-molecule superpositions[14]. These Feshbach molecules and their creation process are also important for understanding ultracold fermionic systems in the BCS-BEC crossover regime because they are closely related to the pairing mechanism in a fermionic superfluid that occurs near a Feshbach resonance[15, 16, 17, 18]. We study the process of production of ultracold molecules from ultracold atoms using a sinusoidally oscillating magnetic field modulation. The advantage of this method is that it greatly reduces the heating the cloud experiences in the conversion process because the conversion occurs far from the center of the Feshbach resonance. In recent experiments, this technique has been applied and was shown could produce molecules from atoms more efficiently[19] and measure the binding energy of Feshbach molecule precisely. However, the underlying mechanism is not fully understood, the complexity arises from the many-body problem and time-dependent field involved. The many experimental observations can not be accounted for by the existing theoretical model. For example, the Poisson distribution predicted by theory[20] is departure from the observed Lorentzian-like resonance profiles and how the finite-temperature effect influences the resonance profiles is still an open problem. In the present paper, we exploit a microscopic two-channel model to investigate thoroughly the mechanism underlying the Shapiro resonance phenomenon in the atom-molecule conversion. With quantitatively considering the thermal dephasing effect in the uncondensed atom clouds our model could account for the most experimental observations. Our theory also suggests some interesting predictions for future's experimental test.

The plan of this paper is as follows. In Sec. II we present our model and make a thorough analysis on the Shapiro resonance. In Sec. III, with the inclusion of the

*Electronic address: liu'jie@iapcm.ac.cn

dephasing effect in our model, we apply our theory to explain the recent experiment. In Sec. IV, we extend to discuss the Shapiro resonance for the case of condensed atoms with emphasizing on the influence from the interaction between coherent particles. Sec. V is our conclusion.

II. SHAPIRO-LIKE RESONANCE IN ATOM-MOLECULE CONVERSION FROM A TWO-CHANNEL PERSPECTIVE

A. Model

Ignoring the two- and three-body atomic decay and collisional molecular decay, we exploit the following two-channel microscopic model to describe the dynamics of converting atoms to molecules in the bosonic system,

$$\hat{H} = (\epsilon_a - \mu) \hat{a}^\dagger \hat{a} + (\epsilon_b + \nu(t) - 2\mu) \hat{b}^\dagger \hat{b} + \frac{g}{\sqrt{\mathcal{V}}} (\hat{a}^\dagger \hat{a}^\dagger \hat{b} + \hat{b}^\dagger \hat{a} \hat{a}). \quad (1)$$

Here \hat{a} (\hat{a}^\dagger) and \hat{b} (\hat{b}^\dagger) are bose annihilation (creation) operators of atoms and molecules, respectively. The total number of particles $N = \hat{a}^\dagger \hat{a} + 2\hat{b}^\dagger \hat{b}$ is a conserved constant. The atomic and molecular kinetic energies are given by ϵ_a and ϵ_b , μ is the chemical potential, g governs the atom-molecule coupling strength, \mathcal{V} denotes the quantization volume of trapped particles and therefore $n = N/\mathcal{V}$ is the mean density of initial bosonic atoms. Where $\nu(t)$ represents the binding energy of diatomic molecules which depends on the external field, expressed approximately as[21],

$$\nu(t) = -\frac{\hbar^2}{m(a_{eff} - r_0)^2}, \quad (2)$$

where r_0 is the effective range of the van der Waals potential, m is the mass of a bosonic atom, and a_{eff} denotes the effective scattering length driven by external magnetic field,

$$a_{eff} = a_{bg} \left(1 - \frac{\Delta B}{B - B_0}\right), \quad (3)$$

where a_{bg} is the background scattering length, B_0 is the Feshbach resonance position, ΔB is the width of the resonance defined through the relation with the atom-molecule coupling term $\Delta B = mg^2/4\pi\hbar^2|a_{bg}\Delta\mu|$, where $\Delta\mu$ is the difference in magnetic moment between the closed channel and the open channel state. We focus on the situation that the selected external field B_{ex} is modulated sinusoidally with small amplitude B_{mod} and large frequency ω near a Feshbach resonance, i.e.,

$$B(t) = B_{ex} + B_{mod} \sin(\omega t). \quad (4)$$

Since $B_{mod} \ll B_{ex}$, the binding energy can be expanded into series to the first order of B_{mod}

$$\nu(t) = \nu_e + \nu_m \sin(\omega t), \quad (5)$$

where

$$\nu_e = -\frac{\hbar^2}{ma_{bg}^2} \frac{(B_{ex} - B_0)^2}{\left[\left(1 - \frac{r_0}{a_{bg}}\right)(B_{ex} - B_0) - \Delta B\right]^2}, \quad (6)$$

and

$$\nu_m = \frac{\hbar^2}{ma_{bg}^2} \frac{2(B_{ex} - B_0)\Delta BB_{mod}}{\left[\left(1 - \frac{r_0}{a_{bg}}\right)(B_{ex} - B_0) - \Delta B\right]^3}. \quad (7)$$

B. Shapiro-like resonance

We introduce the angular momentum operators to investigate the dynamics of this system[22],

$$\hat{L}_x = \sqrt{2} \frac{\hat{a}^\dagger \hat{a}^\dagger \hat{b} + \hat{b}^\dagger \hat{a} \hat{a}}{N^{3/2}}, \quad (8)$$

$$\hat{L}_y = \sqrt{2}i \frac{\hat{a}^\dagger \hat{a}^\dagger \hat{b} - \hat{b}^\dagger \hat{a} \hat{a}}{N^{3/2}}, \quad (9)$$

$$\hat{L}_z = \frac{2\hat{b}^\dagger \hat{b} - \hat{a}^\dagger \hat{a}}{N}, \quad (10)$$

with the commutators

$$[\hat{L}_z, \hat{L}_x] = \frac{4i}{N} \hat{L}_y, \quad (11)$$

$$[\hat{L}_z, \hat{L}_y] = -\frac{4i}{N} \hat{L}_x, \quad (12)$$

$$[\hat{L}_x, \hat{L}_y] = \frac{i}{N} (1 - \hat{L}_z) (1 + 3\hat{L}_z) + \frac{4i}{N^2}. \quad (13)$$

Then the Hamiltonian can be written as

$$H = \frac{N}{4} \left((\nu_0 + \nu_m \sin(\omega t)) \hat{L}_z + \sqrt{2}\eta \hat{L}_x \right), \quad (14)$$

where $\nu_0 = \nu_e + \epsilon_b - 2\epsilon_a$ is the energy difference between atoms and molecules, and parameter $\eta = 2g\sqrt{n}$ denotes the coupling strength. Then the Heisenberg equations of motion are

$$\frac{d}{dt} \hat{L}_x = -\frac{1}{\hbar} (\nu_0 + \nu_m \sin(\omega t)) \hat{L}_y, \quad (15)$$

$$\begin{aligned} \frac{d}{dt} \hat{L}_y &= \frac{1}{\hbar} (\nu_0 + \nu_m \sin(\omega t)) \hat{L}_x - \frac{\eta\sqrt{2}}{\hbar N} \\ &\quad + \frac{\eta 3\sqrt{2}}{\hbar 4} (\hat{L}_z - 1) \left(\hat{L}_z + \frac{1}{3} \right), \end{aligned} \quad (16)$$

$$\frac{d}{dt} \hat{L}_z = \frac{\eta}{\hbar} \sqrt{2} \hat{L}_y. \quad (17)$$

Since N is large for the current experiments and all the commutators vanish in the limit of $N \rightarrow \infty$, it is appropriate to take L_x , L_y , and L_z as three real numbers u , v , w , respectively. Then we get the mean-field Heisen-

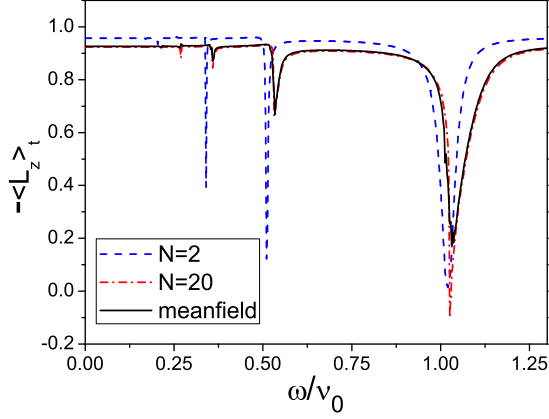


FIG. 1: Time-averaged population imbalance $-\langle\hat{L}_z\rangle_t$ for the driven system with different numbers of particles, tilt $\nu_0/\eta = 5$, and scaled driving amplitude $\nu_m = 1$.

berg equations

$$\frac{d}{dt}u = -\frac{1}{\hbar}(\nu_0 + \nu_m \sin(\omega t))v, \quad (18)$$

$$\frac{d}{dt}v = \frac{1}{\hbar}(\nu_0 + \nu_m \sin(\omega t))u + \frac{\eta}{\hbar} \frac{3\sqrt{2}}{4}(w-1)\left(w + \frac{1}{3}\right), \quad (19)$$

$$\frac{d}{dt}w = \frac{\eta}{\hbar}\sqrt{2}v. \quad (20)$$

In order to get the time-averaged value of the conversion varied with different external field, we characterize each quantum trajectory by its time-averaged imbalance

$$-\langle\hat{L}_z\rangle_t \equiv -\frac{1}{\Delta t} \int_0^{\Delta t} dt \langle\hat{L}_z\rangle(t), \quad (21)$$

employing the averaging interval $\Delta t \gg \hbar/\nu_0$. Initially, all particles are atoms. Fig.1 shows the results of such calculations by numerical solving the Heisenberg equations(15-17) for $N = 2, 20$ under periodic modulation with fixed scaled amplitude $\nu_m/\nu_0 = 0.2$ and frequencies ω ranging from 0 to $1.25\nu_0$. The solution of the mean-field equations (18-20) is also presented. There are several clear spikes which indicate the Shapiro-like resonance in atom-molecule conversion driven by external magnetic field.

These spikes indicate that the frequency of the modulated field is commensurate with the intrinsic frequencies of the atom-molecule conversion system in the absence of the periodic modulation. Now we analyze the intrinsic frequency. For $N = 2$, using Fock state as basis, the commutators (11-13) becomes

$$[\hat{L}_z, \hat{L}_x] = 2i\hat{L}_y, \quad [\hat{L}_z, \hat{L}_y] = -2i\hat{L}_x, \quad (22)$$

$$[\hat{L}_x, \hat{L}_y] = i\hat{L}_z. \quad (23)$$

From the Heisenberg equations(15-17), we get

$$\frac{d^2}{dt^2}\hat{L}_y + \frac{1}{\hbar^2}(\nu_0^2 + \eta^2)\hat{L}_y = 0. \quad (24)$$

Then the intrinsic frequency is readily obtained from the above equation as $\sqrt{\nu_0^2 + \eta^2}/\hbar$. So the center of resonance is expected to be $\sqrt{\nu_0^2 + \eta^2}/(\hbar\omega) = p/q$ with p, q are integers. In our case, the resonances corresponding to $p/q = 1, 2, 3$ are more prominent. With N increasing, we find that the resonance center shifts to right due to the many-body effect. We can obtain the intrinsic frequency in the mean-field limit, i.e., $N \rightarrow \infty$. From the mean-field equations(18-20) we readily obtain,

$$\frac{d^2}{dt^2}v + \frac{1}{\hbar^2}(\nu_0^2 + \eta^2(1 - 3w))v = 0, \quad (25)$$

Initially all particles are in atom states, i.e., $w = -1$. Approximately substituting it into the above equation we obtain the explicit expression of the frequency $\sqrt{\nu_0^2 + 4\eta^2}/\hbar$. It implies that due to the many-body effect[23], the resonance centers shifts to $\sqrt{\nu_0^2 + 4\eta^2}/(\hbar\omega) = 1, 2, 3, \dots$. The above theoretical analysis agree with our numerical results.

C. Phase space at the Shapiro-like resonance

The Shapiro resonance phenomenon can be demonstrated intuitively by the trajectories in phase space of the system. Notice that the constraint $u^2 + v^2 = \frac{1}{2}(w-1)^2(w+1)$ and introducing the canonical variable $s = w$, $\theta = \arctan(v/u)$ denoting the population imbalance and the relative phase between atoms and molecules, the mean-field Heisenberg equations can be replaced by a classical Hamiltonian of the form

$$\mathcal{H} = \frac{1}{\hbar}(\nu_0 + \nu_m \sin(\omega t))s + \frac{\eta}{\hbar}\sqrt{(s-1)^2(s+1)}\cos\theta, \quad (26)$$

the canonical equations of motions are

$$\frac{d\theta}{dt} = \frac{\partial\mathcal{H}}{\partial s} = \frac{1}{\hbar}(\nu_0 + \nu_m \sin(\omega t)) - \frac{\eta}{\hbar} \frac{(1+3s)}{2\sqrt{1+s}}\cos\theta \quad (27)$$

$$\frac{ds}{dt} = -\frac{\partial\mathcal{H}}{\partial\theta} = \frac{\eta}{\hbar}\sqrt{(1-s)^2(1+s)}\sin\theta. \quad (28)$$

Using a generation function

$$F(\theta, S) = \left(\theta - \frac{\nu_0 t}{\hbar} + \frac{\nu_m}{\hbar\omega}\cos(\omega t)\right)S, \quad (29)$$

with following relations

$$s = \frac{\partial F}{\partial\theta} = S, \quad (30)$$

$$\Theta = \frac{\partial F}{\partial S} = \left(\theta - \frac{\nu_0 t}{\hbar} + \frac{\nu_m}{\hbar\omega}\cos(\omega t)\right), \quad (31)$$

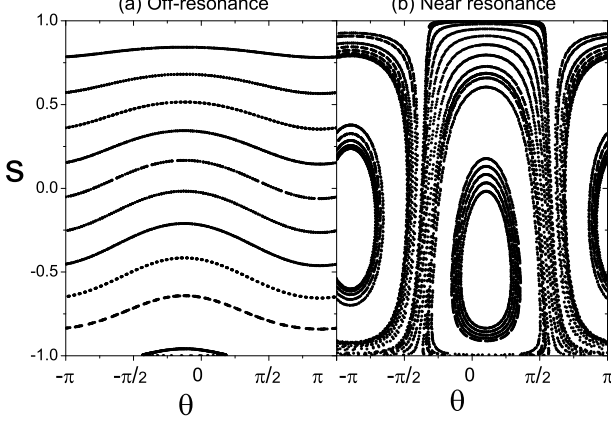


FIG. 2: Poincaré section of the classical Hamiltonian (26) with tilt $\nu_0/\eta = 24$, scaled driving amplitude $\nu_m = 0.2\nu_0$, and modulation frequency (a) $\omega/\nu_0 = 0.95$ (off-resonance), (b) $\omega/\nu_0 = 1$ (near resonance).

we obtain the new Hamiltonian

$$\begin{aligned} \mathcal{K}(S, \Theta) &= \mathcal{H} + \frac{\partial F}{\partial t} \\ &= \frac{\eta}{\hbar} \sqrt{(1-S)^2(1+S)} \\ &\quad \cos \left(\Theta + \frac{\nu_0 t}{\hbar} - \frac{\nu_m}{\hbar \omega} \cos(\omega t) \right). \end{aligned} \quad (32)$$

The secular evolution of S and Θ can be evaluated from the time-averaged Hamiltonian,

$$\langle \mathcal{K}(S, \Theta) \rangle_T = \frac{1}{T} \int_0^T \mathcal{K}(S, \Theta) dt, \quad (33)$$

with $T = 2\pi/\omega$.

Now, we consider the 1:1 resonance case that $\hbar\omega \approx \nu_0$,

$$\langle \mathcal{K}(S, \Theta) \rangle_T \approx J_1\left(\frac{\nu_m}{\nu_0}\right) \frac{\eta}{\hbar} \sqrt{(1-S)^2(1+S)} \sin \Theta. \quad (34)$$

where $J_1(x)$ is the first kind Bessel function. The phase graph of the periodic averaged Hamiltonian system reflects the Poincaré section of Hamiltonian system (26), as shown in Fig.2. For the case of off-resonance, the integral in Eq.(33) approximates to zero, it implies that the time-averaged s varies a little in time while the variable θ increases with time almost linearly. The corresponding Poincaré section is shown in Fig.2(b). It is shown that the phase space at the transition change dramatically.

D. Intrinsic resonance width: Arnold tongues

For the initial condition $s = w = 1$, whether its trajectory falls into resonance regime can be judged from following resonance condition $\Delta\mathcal{H} > 2\nu_0/\hbar$, where $\Delta\mathcal{H}$ is

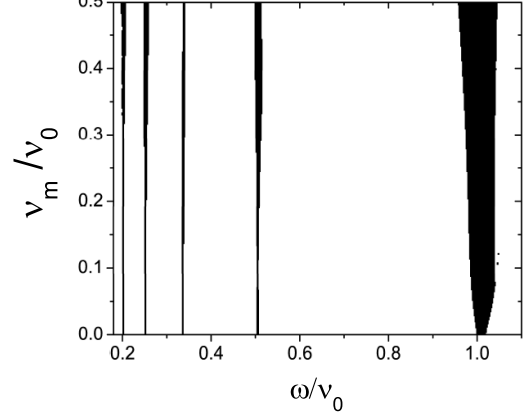


FIG. 3: Arnold tongues for resonance modes (1 : 1), (2 : 1), (3 : 1), (4 : 1), (5 : 1) (from right to left) with $\nu_0/\eta = 5$.

the difference between the maximum and the minimum value of \mathcal{H} in the time interval $\Delta t \gg \hbar/\nu_0$. For different ν_m and ω , we obtain the regions in the two-dimensional parameter space where the resonance emerges. These regions are named as Arnold tongues[24]. In order to draw out the Arnold tongues in parameter space, the main numerical tool used in this work is the winding number \mathcal{W}

$$\mathcal{W} = \lim_{t \rightarrow \infty} \frac{\theta(t) - \theta(0)}{t}. \quad (35)$$

with initial conditions $(\theta(0), s(0))$. If the ratio \mathcal{W}/ω is rational, i.e., $\mathcal{W}/\omega = q/p$, here q and p are natural number, $(\theta(t), s(t))$ is a resonant solution of $(q : p)$ type, i.e.,

$$(\theta(t + pT), s(t + pT)) = (\theta(t), s(t)) + (2\pi q, 0), \quad (36)$$

which means the system runs q times in time pT interval. In our system, only $(q : 1)$ type is significant. In Fig.3 we show the first five resonance regions with $\nu_0/\eta = 5$. The width of the resonance regions is broadened as the modulation amplitude ν_m increases.

III. COMPARISON WITH EXPERIMENT

In the above discussion we use the single-mode model to discuss the conversion between the condensed atoms and molecules. This is an approximation because in practical experiments the atoms are not condensed and other modes will be coupled. We use this approximation under the condition that the energy distribution of the thermal particles (characterized by $k_B T$, k_B is the Boltzmann constant and T is the temperature) is much smaller than the effective Feshbach resonance width $g\sqrt{n}$ [23]. In such cases, each 'energy band' of the thermal particles can be approximately denoted by one energy level, as schematically plotted by Fig.4. Initially, the particles

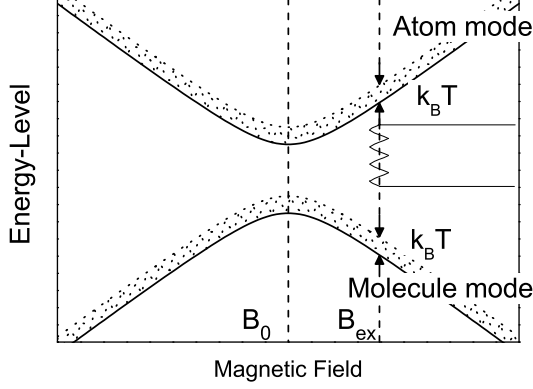


FIG. 4: Schematic of the swept magnetic field in experiment. See text for details.

on one level have a definite phase and the phase difference between two levels is well defined. However, as the magnetic field sweeps and then the sinusoidal magnetic field applied, particles will acquire additional phases that are proportional to their individual energy and evolution time. The varied particles in one level could acquire different phases because they have different energies. This define a 'dephasing rate' $\gamma = k_B T / (2\pi\hbar)$ [23]. To compare with experiment, we need to include the dephasing effect into our model. Modeling dephasing by fully include the quantum effects requires sophisticated theoretical studies. The standard approaches of quantum optics for open systems involve quantum kinetic master equations. Here, we adopt the simple mean-field treatment in our model. From the mean-field viewpoint, the decoherence term introduces a γ transversal relaxation term into the mean-field equations of motion[25],

$$\frac{d}{dt}u = -\frac{1}{\hbar}(\nu(t) + \epsilon_b - 2\epsilon_a)v - \gamma u, \quad (37)$$

$$\begin{aligned} \frac{d}{dt}v &= \frac{1}{\hbar}(\nu(t) + \epsilon_b - 2\epsilon_a)u \\ &+ \frac{\eta}{\hbar} \frac{3}{4} \sqrt{2} (w - 1) \left(w + \frac{1}{3} \right) - \gamma v, \end{aligned} \quad (38)$$

$$\frac{d}{dt}w = \frac{\eta}{\hbar} \sqrt{2} v, \quad (39)$$

The imbalance of atom-pairs and molecules w is varied in the range of $[-1, 1]$ with the lower limit corresponding to a pure atomic gas and $w = 1$ for a pure molecular gas. What we concern is that after the conversion process how many atomic pairs are converted to molecule. We use w_f to denote the value of w when the magnetic field sweep back. The molecular conversion efficiency can be read from the variable w_f as $\Gamma = (1 + w_f)/2$.

Now we apply our theory to the experiment of ^{85}Rb by Ref.[19]. The atoms are held in a purely magnetic trap at a bias field of B_r . After evaporative cooling, the

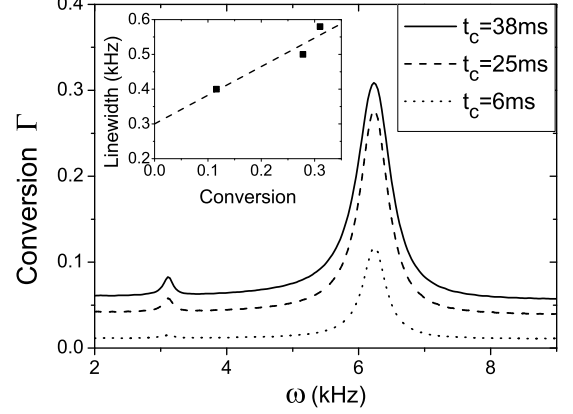


FIG. 5: Conversion efficiency of atoms converted to molecules as a function of modulation frequency for three different coupling times. For a fixed coupling time, the curve can be fitted by a Lorentzian distribution $\Gamma = \Gamma_0 + \frac{2A}{\pi} \frac{\Delta}{4(\omega - \omega_c)^2 + \Delta^2}$, e.g., for $t_c = 38\text{ms}$, the fitting parameters are $\Gamma_0 = 0.06$, $\omega_c = 6.2$, $\Delta = 0.6$, $A = 0.23$. In the subfigure, by fitting the linewidth versus conversion data to a straight line we find the zero conversion limit to be 0.3kHz .

magnetic field B is linearly swept to a selected value at B_{ex} and then apply a sinusoidal magnetic field pulse with peak-to-peak amplitude B_{mod} and modulation frequency ω for a duration of coupling time. The swept magnetic

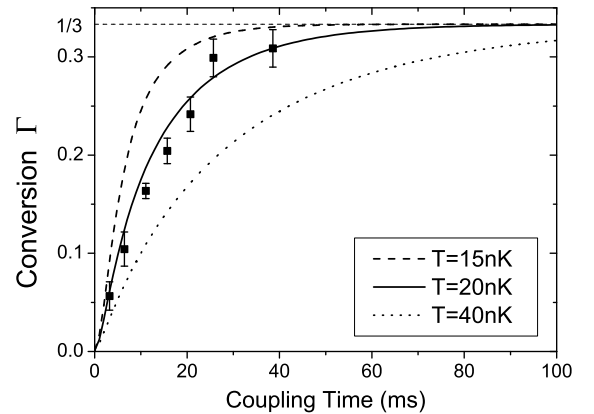


FIG. 6: Conversion efficiency of atoms converted to molecules under a periodic modulation with amplitude $B_{mod} = 0.13G$ and frequency $\omega = 6.25\text{kHz}$ with respect to coupling time for different temperatures. The conversion of ultracold atoms to molecules increases with coupling time until it becomes saturated at $1/3$.

field can be expressed as

$$B = \begin{cases} B_r - \alpha t & 0 \leq t < t_0 \\ B_{ex} + B_{mod} \sin(\omega t) & t_0 \leq t < t_0 + t_c \\ B_{ex} + \alpha t & t_0 + t_c \leq t < 2t_0 + t_c. \end{cases} \quad (40)$$

Where $B_r = 162G$, $B_{ex} = 156.5G$, $B_{mod} = 0.13G$, ω is ranging from $2kHz$ to $9kHz$, t_0 is the linear sweep time, $\alpha = (B_r - B_{ex})/t_0$ is the linear sweep rate, and t_c is the coupling time. The sketch curve is shown in Fig.4. For the thermal cloud, with temperature T , one molecule have 5 degrees of freedom while two atoms have 6 degrees of freedom, according to the equipartition theorem, we have $(2\epsilon_a - \epsilon_b) \approx k_B T/2$. The scaled parameters in Eq.(37-39) are

$$\nu(t) = -\frac{\hbar^2}{ma_{bg}^2} \frac{(B - B_0)^2}{\left[\left(1 - \frac{r_0}{a_{bg}}\right) (B - B_0) - \Delta B \right]^2}, \quad (41)$$

and

$$\eta = 2\sqrt{4\pi\hbar^2 |a_{bg}| \Delta\mu |\Delta B n/m}. \quad (42)$$

The experimental parameters are $a_{bg} = -443a_0$, $r_0 = 185a_0$ [26], $\Delta B = 10.71G$, $B_0 = 155G$, $\Delta\mu = 1.2 \times 10^{-4}\mu_B$, the temperature $T = 20nK$, density $n = 10^{11}cm^{-3}$, here a_0 and μ_B are Bohr radius and Bohr magneton, respectively. The difference of magnetic moment $\Delta\mu$ is extracted from the experimental data[27]. Under this condition, the ratio between the energy difference and the energy distribution of thermal particles, i.e., $\nu_e/k_B T$, is estimated to be around 15 that is much larger than one. The above analysis validates our single mode approximation. Fig.5 shows the conversion efficiency as a function of modulation frequency for three different coupling times. The resonance line width are broadened by the dephasing term. There is a clear Lorentzian distribution resonance at frequency about $6.25kHz$, close to experiment. Except the fundamental frequency resonance at $\omega = 6.25kHz$, there is also a weakly (2 : 1) mode resonance at about $\omega = 3.1kHz$, while it has not been observed in experiment. Our linewidth is approximately $0.3kHz$ at zero conversion limit, as shown in the subfigure. In the experiment, it is about $0.2kHz$.

In our calculation, we find that, in the three stages of magnetic field change expressed by Eq.(40), the linear process contributes little to the atom-molecule conversion. This is because oscillation center B_{ex} is still far away from the Feshbach resonance center. The atom-molecule conversion mainly occurs in the process of applying the sinusoidal magnetic field, where $\nu(t)$ can be expressed as $\nu_0 + \nu_m \sin(\omega t)$. Therefore, the above observed resonance phenomenon corresponds to the Shapiro resonance discussed in the last section, while the linewidth is dramatically broadened by the thermal dephasing effect.

In Fig.6, we show the conversion efficiency with respect to coupling time. For temperature $T = 20nK$, density $n = 10^{11}cm^{-3}$, our results are close to experimental

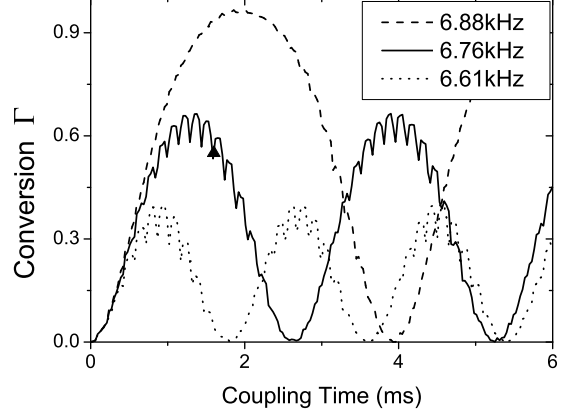


FIG. 7: The conversion efficiency from condensed atoms to molecules under a periodic modulation with fixed amplitude $B_{mod} = 0.5G$ and different frequencies. The density for the condensed atoms is $n = 10^{12}cm^{-3}$. The dark triangle marks the experimental observation in Ref.[19].

data. We also show the cases of different temperatures by considering the isobaric condition, i.e., $nT = const..$ The above calculation shows that increasing the temperature will lessen the molecular production because the dephasing term is proportional to temperature. On the other aspect, the conversion efficiency decreases with the increasing of temperature. For different temperature, a common feature is that the conversion efficiency increases with coupling time until it becomes saturated at $1/3$. This can be explained from investigating Eq.(37-39), where $u = v = 0, w = -1/3$ is the fixed point in the absence of the dephasing term. In the presence of the dephasing effect, the system is expected to relax into the fixed point in the case of long-term coupling.

IV. DYNAMICS OF ATOM-MOLECULE CONVERSION FOR THE CONDENSED ATOMS

In this section, we extend our discussion to the case of condensed atoms. For pure BEC atoms, the single mode approximation is valid and dephasing effect can be ignored while the interaction between the coherent atoms become significant. After ignoring the kinetic energies of particles, the Hamiltonian can be written as

$$\hat{H} = \nu(t)\hat{b}^\dagger\hat{b} - \frac{U}{V}\hat{a}^\dagger\hat{a}^\dagger\hat{a}\hat{a} + \frac{g}{\sqrt{V}}\left(\hat{a}^\dagger\hat{a}^\dagger\hat{b} + \hat{b}^\dagger\hat{a}\hat{a}\right). \quad (43)$$

where $U = 4\pi\hbar^2|a_{bg}|/m$ denotes the nonlinear interaction. In mean-field limit, we can derive the Heisenberg

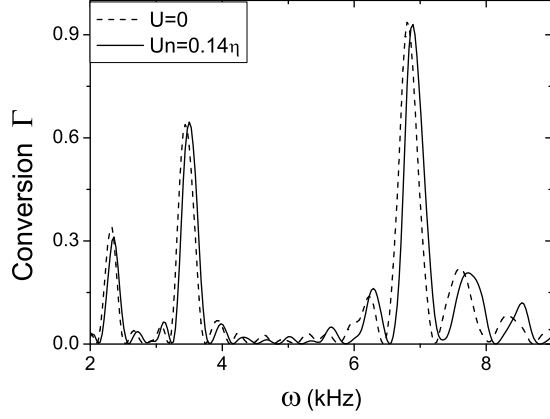


FIG. 8: The conversion efficiency from condensed atoms to molecules with respect to modulation frequency for different nonlinear interaction U . The coupling time is $1.6ms$. The other parameters are the same as in Fig.7.

equations of motion

$$\frac{d}{dt}u = -\frac{\nu(t)}{\hbar}v - \frac{2Un}{\hbar}v(1-w), \quad (44)$$

$$\begin{aligned} \frac{d}{dt}v &= \frac{\nu(t)}{\hbar}u + \frac{\eta}{\hbar}\frac{3}{4}\sqrt{2}(w-1)\left(w + \frac{1}{3}\right) \\ &\quad + \frac{2Un}{\hbar}u(1-w), \end{aligned} \quad (45)$$

$$\frac{d}{dt}w = \frac{\eta}{\hbar}\sqrt{2}v. \quad (46)$$

Fig.7 presents the conversion efficiency under a periodic modulation with fixed amplitude $B_{mod} = 0.5G$ and different frequencies by numerical solving Eq.(44-46). The density for the condensed atoms is $n = 10^{12}cm^{-3}$ and thereby the scaled nonlinear interaction is $Un/\eta =$

0.14. One sees that there is a Rabi oscillation which can reach a high conversion efficiency. In experiment, they observe 55% conversion for coupling time $1.6ms$ [19]. The observation marked by a dark triangle in Fig.7 is consistent with our result. Fig.8 presents the conversion efficiency with respect to modulation frequency for different nonlinear interaction U . The coupling time for this calculation is $1.6ms$. The other parameters are the same as in Fig.7.

In Fig.8, we observe some oscillations except for the main resonance peaks and find that the maximum conversion efficiency could be far beyond the limit $1/3$. Because the resonance center can be still approximated by $\omega = \sqrt{\nu_e^2 + 4\eta^2}/\hbar$. It implicitly depends on the density through parameter η . In the experiment, the density of condensed atoms is about ten times larger than that of thermal cloud, therefore the resonance center shift to the right-hand compared to Fig.5 of the thermal atomic cloud case. Moreover, we find that the interaction between the coherent atoms will lead to the shift of the resonance profile as clearly shown in Fig.8.

V. CONCLUSIONS

In conclusion, we have investigated thoroughly the mechanism underlying the Shapiro resonance phenomenon in the atom-molecule conversion with exploiting a microscopic two-channel model. With the inclusion of the thermal dephasing effect in the uncondensed atom clouds our model could account for the most experimental observations. We also extend our discussions to the case of condensed atoms. Our theory have some interesting predictions waiting for future's experimental test.

This work is supported by National Natural Science Foundation of China (No.10725521,10604009), 973 project of China under Grant No. 2006CB921400, 2007CB814800.

-
- [1] S. Shapiro, Phys. Rev. Lett. **11**, 80 (1963).
 - [2] A. Barone and G. Paternò, *Physics and Applications of the Josephson Effect* (Wiley, New York, 1982).
 - [3] F. Bloch, Phys. Rev. B **2**, 109 (1970).
 - [4] T. A. Fulton, Phys. Rev. **7**, 981 (1973).
 - [5] B. N. Taylor, W. H. Parker, D. N. Langenberg, and A. Denestein, Metrologia **3**, 89 (1967).
 - [6] R. Pöpel, Metrologia **29**, 153 (1992).
 - [7] S. Raghavan, A. Smerzi, S. Fantoni, and S. R. Shenoy, Phys. Rev. A **59**, 620 (1999).
 - [8] André Eckardt, Tharanga Jinasundera, Christoph Weiss, and Martin Holthaus, Phys. Rev. Lett. **95**, 200401 (2005).
 - [9] Sigmund Kohler and Fernando Sols, New J. Phys. **5**, 94 (2003).
 - [10] M. Greiner, C. A. Regal, and D. S. Jin, Nature (London) **426**, 537 (2003).
 - [11] M. W. Zwierlein, C. A. Stan, C. H. Schunck, S. M. F. Raupach, S. Gupta, Z. Hadzibabic, and W. Ketterle, Phys. Rev. Lett. **91**, 250401 (2003).
 - [12] S. Jochim, M. Bartenstein, A. Altmeyer, G. Hendl, S. Riedl, C. Chin, J. Hecker Denschlag, R. Grimm, Science **302**, 2101 (2003).
 - [13] M. Bartenstein, A. Altmeyer, S. Riedl, S. Jochim, C. Chin, J. Hecker Denschlag, and R. Grimm, Phys. Rev. Lett. **92**, 120401 (2004).
 - [14] E.A. Donley, N.R. Claussen, S.T. Thompson, and C.E. Wieman, Nature (London) **417**, 529 (2002).
 - [15] M. Holland, S.J.J.M.F. Kokkelmans, M.L. Chiofalo, and R. Walser, Phys. Rev. Lett. **87**, 120406 (2001).
 - [16] E. Timmermans, K. Furuya, P.W. Milloni, and A.K. Kerman, Phys. Lett. A **285**, 228 (2001).
 - [17] M. W. Zwierlein, C. A. Stan, C. H. Schunck, S. M. F. Raupach, A. J. Kerman, and W. Ketterle, Phys. Rev.

- Lett. **92**, 120403 (2004).
- [18] M. Greiner, C.A. Regal, and D.S. Jin, Phys. Rev. Lett. **94**, 070403 (2005).
 - [19] S. T. Thompson, E. Hodby, and C. E. Wieman, Phys. Rev. Lett. **95**, 190404 (2005).
 - [20] Thomas M. Hanna, Thorsten Köhler, and Keith Burnett, Phys. Rev. A. **75**, 013606 (2007).
 - [21] Thorsten Köhler, and Krzysztof Góral, Rev. Mod. Phys. **78**, 1311 (2006).
 - [22] A. Vardi, V. A. Yurovsky, and J. R. Anglin, Phys. Rev. A. **64**, 063611 (2001).
 - [23] Jie Liu, Bin Liu, Libin Fu, Phys. Rev. A **78**, 013618 (2008).
 - [24] V. I. Arnold, Trans. Am. Math. Soc., Ser. 2 **46**, 213 (1965);
 - [25] Jie Liu, Chuanwei Zhang, Mark G. Raizen, and Qian Niu, Phys. Rev. A **73**, 013601 (2006).
 - [26] R A Duine, and H T C Stoof, New J. Phys. **5**, 69 (2003); G. F. Gribakin, and V. V. Flambaum, Phys. Rev. A **48**, 546 (1993).
 - [27] N. R. Claussen, S. J. J. M. F. Kokkelmans, S. T. Thompson, E. A. Donley, E. Hodby, and C. E. Wieman, Phys. Rev. A. **67**, 060701(R) (2003).